SINGLE-CHANNEL ACETYLCHOLINE RECEPTOR KINETICS

MARK D. LEIBOWITZ AND VINCENT E. DIONNE
Departments of Biology and Medicine, University of California at San Diego, La Jolla, California 92093

ABSTRACT The temporal relationships among junctional acetylcholine receptor single-channel currents have been examined to probe the mechanism of channel activation. We have presented an analytical approach, termed single-channel ensemble analysis, that allows one to estimate the kinetic transition rate constants for channel-opening and closing as well as the rate of leaving the specific doubly-liganded, closed state from which opening occurs. This approach may be applied to data produced by any number of independent channels as long as the probability of channel opening is low, a condition that is experimentally verifiable. The method has been independently validated using simulated single-channel data generated by computer from one or 100 hypothetical channels. Typical experimental values for the transition rate constants estimated from acetylcholine-activated single channels at the garter snake neuromuscular junction were: opening = 1,200 s^{-1}, closing = 455 s^{-1}, back rate for leaving the doubly-liganded, closed state = 3,200 s^{-1} at a transmembrane potential of −92 mV at room temperature. Each of these three rate constants was voltage dependent, with the closing rate decreasing *e*-fold for 173 mV of hyperpolarization, the opening rate increasing *e*-fold for 78 mV, and the unbinding rate increasing *e*-fold for 105 mV. The channel-closing rate was agonist dependent, being greater at all potentials for channels activated with carbamylcholine than for channels activated with acetylcholine. However, the single-channel conductance and reversal potential were the same for these two agonists.

INTRODUCTION

The nicotinic acetylcholine receptor (AChR) transduces a chemical signal into electrical activity at neuromuscular junctions on vertebrate skeletal muscle (1). When acetylcholine (ACh) binds to a receptor, the associated membrane channel can open, allowing cations to flow into the cell; this transmembrane current initiates the cascade of events leading to muscle contraction. The fundamental role of this transduction process, by which the binding of ACh to the receptor affects the opening of ion channels, makes understanding the mechanism of AChR function an important problem for physiologists.

The current flowing through AChR channels is a parameter which can be measured and used to probe the mechanism of receptor function (2, 3). Until recently this type of work has relied upon measurements of the ensemble behavior of large populations of receptor channels made using the voltage clamp. In general, the responses recorded in those studies were fit with an apparent rate that was interpreted as the rate of channel closing (4, 5). Although under certain circumstances the channel-closing rate dominated this apparent rate, the individual transition rate constants were not directly measured.

Significantly more detailed kinetic behavior of the AChR channel can be resolved using the patch-clamp technique to record single-channel activity (6, 7). Single-channel recordings are a sensitive record of the temporal behavior of individual channels and can be analyzed mathematically to provide estimates of the transition rate constants for a given model of receptor activation. This theoretical problem has been dealt with elegantly by Colquhoun and Hawkes (8) for records in which apparent bursts of activity from one channel can be unambiguously identified and separated from other activity. This condition is difficult to verify, because it is formally satisfied only when a patch contains a single ion channel. Although this analysis has been applied to patches that contain several channels (9), at the neuromuscular junction, where the density of AChR channels is very high, it is impossible to separate the activity of one channel from another; the approach presented by Colquhoun and Hawkes is thus not applicable.

In an earlier paper we described a quantitative method for the systematic evaluation of ion-channel kinetics from single-channel measurements, a method we call single-channel ensemble analysis. To apply this analysis, the essential kinetic information contained in a recording of channel activity is reformulated as a set of histograms. These histograms are actually probability functions that have been experimentally evaluated independent of any model for the receptor. Their value is that they may be fit

Dr Leibowitz's current address is the Department of Physiology and Biophysics, University of Washington, Seattle, WA. Address reprint requests to Dr. Dionne.

with mathematical predictions derived from plausible kinetic models of receptor behavior. This allows kinetic models to be tested for applicability and the transition rate constants of accurate models to be evaluated.

An example will illustrate some of these concepts. Consider the single-channel open-duration histogram, which is one of a set of histograms that can be constructed to study channel behavior. It can be described more precisely as a histogram of times at which a given channel closes after opening (the data being confined to single events); this histogram is an experimental measure of the time-dependent probability with which a channel closes, once opened. The open-duration histogram contains just a fraction of the kinetic information contained in a single-channel recording, revealing only the rate of channel closing with no indication of how rapidly the channel opens or how it proceeds through transient closed states. To examine these properties, other histograms of channel activity can be constructed.

The histograms, as experimental measures of probability, provide a connection between models of receptor behavior and the raw data record. Kinetic models are easily treated mathematically to predict the probability of any sequence of transitions among the states, and these predictions may be directly compared with the appropriate histograms. In addition, general principles may be applied to simplify model selection, so that large classes of kinetic models may be discarded by inspection. Consider the example of the open-duration distribution. All models containing a single open channel state predict that the open-duration histogram will decay exponentially with time, regardless of the number of closing paths and the complexity of interrelations. However, models with several open states necessarily predict more complicated open-duration distributions. Thus, inspection of the open-duration histogram might allow one of these classes of models to be discarded. It would be incorrect to fit the simpler models to data from channels with several open states, and the flexibility offered by the more complicated models would be unnecessary for fitting data from channels with one open state. Models must be selected both for the accuracy with which they account for the measured kinetic information and also for their usefulness in describing other channel behavior, e.g., agonist binding.

In many cases single-channel ensemble analysis can be implemented in a manner such that the actual number of channels contributing to a data record is both unknown and unimportant. The essential idea is that at the precise instant when a single open channel closes, leaving all the channels closed, two things are known about the distribution of closed channels: the channel that just closed is in a state directly accessible from the open state, and the remainder of the channels will be distributed on average at equilibrium among all the closed states. This turns out to be a powerful observation, because by constructing histograms which are conditioned upon these special closing transitions we can evaluate the rate of channel opening and the lifetime of the closed state preceeding opening. The reason the precise number of channels is unimportant is that all the histograms portray what is, in essence, the average relaxation time-course for a single channel after a specific perturbation. For the open-duration distribution this perturbation causes the average occupancy of the open-channel state to increment by one; for the other histograms the occupancy of a closed state adjacent to the open state is perturbed, again by one. The mathematical treatment of the kinetic models does assume that the frequency of single-channel activity is low, so that most of the record is comprised of times when zero or just one channel is open. The accuracy of this assumption may be confirmed by inspection of the data.

We have used single-channel ensemble analysis to study the activation kinetics of AChR at the vertebrate neuromuscular junction using a linear four-state kinetic model with macroscopic rate constants.

$$2A + R \underset{k_{-1}}{\overset{k_1}{\rightleftharpoons}} A + AR \underset{k_{-2}}{\overset{k_2}{\rightleftharpoons}} A_2R \underset{\alpha}{\overset{\beta}{\rightleftharpoons}} A_2R^* \qquad (1)$$

Activation is depicted as the sequential binding of two molecules of agonist (A) to the closed receptor (R) followed by a transition to the one open-channel state (A_2R^*). The work was performed at low agonist concentrations so that the association rate constants (ck_1 and ck_2) were small compared with the dissociation rates (k_{-1} and k_{-2}). Many previous whole-cell voltage-clamp measurements have been interpreted using this kinetic scheme or a variant of it (4, 5, 11, 12). Those measurements were usually interpreted as estimates of α, the channel-closing rate constant. Our approach has produced estimates of the rate constants α, β, and k_{-2} from records of channel activity generated at low agonist concentration. Under our experimental conditions, receptor desensitization was negligible, judged by the stationarity of the rate of channel activity and the occasional appearance of multiple open channels.

In this paper we present a qualitative description of single-channel ensemble analysis, an accessment of its accuracy using synthetic data, and results from the AChR channel at garter snake neuromuscular junctions. The specific derivations of the probability functions from scheme 1 can be found in Dionne and Leibowitz (10). These derivations and a quantitative presentation of the single-channel ensemble method were the major content of that earlier report; for illustrative purposes the method was applied to a set of single-channel AChR data recorded at an unknown membrane potential. Because the kinetics of the AChR are strikingly voltage dependent (2–5), the physiological significance of those rate constants could not be evaluated. We report here the results obtained at known membrane voltages.

MATERIALS AND METHODS

Agonist-activated single-channel currents were recorded at junctional regions of garter snake (sp. *Thamnophis*) twitch fiber membrane (13). The costocutaneous muscle, which contains 50–100 individual fibers, was removed intact, along with small sections of the rib and belly scale to which it was attached, and placed in saline containing NaCl 159 mM, KCl 2.15 mM, $CaCl_2$ 1.0 mM, $MgCl_2$ 4.2 mM, HEPES [*N*-2-hydroxyethylpiperazine-*N*'-2-ethanesulfonic acid] 5.0 mM, and tetrodotoxin 100 nM; pH 7.2. The muscle was held to the glass bottom of a plexiglass chamber by stainless steel clips placed near the insertions. The nerve terminal and connective tissue overlying the junctional membrane were removed by incubating the preparation at room temperature (~22°C) in saline containing 2 mg/ml collagenase (form TD, Advance Biofactures Corp., Lynwood, NY) for two hours followed by the addition of 0.09–0.14 mg/ml protease (type XIV from *Streptomyces griseus*, Sigma Chemical Co., St. Louis, MO) for 0.5–1 h. The preparation was then rinsed extensively with saline to remove the enzyme mixture. The enzyme treatment resulted in the lysis of 30%–50% of the cells in most preparations; nevertheless, surviving cells were capable of contracting when depolarized; they appeared undamaged, and could be used for several hours. Exposed regions of AChR-rich junctional membrane, which should contain AChR in high density, were located visually under a compound microscope equipped with Nomarski optics.

Single-channel currents were recorded at room temperature using the "giga-seal" patch-clamp technique as described by others (7). Briefly, pipettes were pulled from flint glass capillaries and their tapered portions coated with Sylgard 182 (Dow Corning Corp., Midland, MI) before the tips were fire-polished. When filled with normal saline, pipette resistance was 3–7 MΩ. Giga-seals could be formed by applying gentle suction to the lumen of the pipette after apposition to the junctional membrane. Agonist was administered at the desired concentration by dissolving it in the saline filling the recording pipettes. Currents flowing across the patch of membrane circumscribed by the pipette were measured using a current-to-voltage converter adapted from a design by Fred Sigworth (7) and built in our laboratory using discrete components. The response of the patch clamp was set to 10 kHz using a single stage of frequency compensation. The compensation was adjusted such that a voltage ramp injected capacitatively at the current-to-voltage converter input produced a square response with the appropriate rise time. The current signal was low-pass filtered at 2.5–5 kHz using a four-pole Bessel filter, and digitally recorded by a laboratory computer (Digital Equipment Corp., Lynwood, MA, model PDP 11/34 or 11/23). Sample intervals, defined as Δt, ranged from 30–100 μs. Records were composed of segments containing 9,216 successive sample points separated by brief intervals during which the computer wrote the segments onto a storage disk.

Analysis of the digitized single-channel current records was performed off-line with the laboratory computers. An operator-assisted search program was used to find and evaluate the amplitude and duration of currents within these records as well as the duration of closed intervals between the events. The search program tracked the mean baseline current and searched for transitions away from the baseline (opening transitions) exceeding a detection threshold for at least two consecutive sample points. After finding a valid opening transition, a closing was sought by searching for a transition toward the baseline that remained below the threshold for at least two consecutive sample points. This threshold was generally set at about one-half the single-channel amplitude (Fig. 1). The data containing each tentative event were displayed along with vectors indicating the computer estimates for the duration and mean amplitude of the open-channel current. Each tentative event was verified and either accepted or rejected by the operator. Whenever the tentative event appeared to contain more than one open channel, the computer was instructed to reanalyze that data using a point-by-point search to locate transitions between the mean current levels. The relative thresholds used to detect these transitions were the same magnitude as those defining unitary events, and again each level had to last a minimum of two sample points. The results of the analysis were saved by the computer as triplets of numbers in a table written onto a storage disk. The triplets recorded open and closed (baseline) durations as well as the current amplitude associated with any open-channel interval. This table fully described the data and could be used to reconstruct the current time course. From these triplets we evaluated the homogeneity and kinetics of the AChR population.

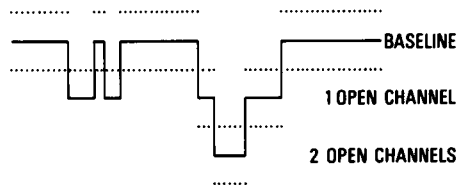

FIGURE 1 Event detection thresholds. Two single-channel events plus one multiple event are shown schematically as solid lines with the appropriate detection thresholds dotted. See text for description.

KINETIC ANALYSIS

Histograms were constructed, using the triplets described above, from which the kinetic transition rate constants for channel opening (β), closing (α), and unbinding from the doubly-liganded, closed state (k_{-2}) were estimated. The three histograms were *a*, the open-duration histogram, a plot of the open times of all single amplitude events; *b*, the first-latency histogram, a plot of the closed (baseline) intervals between open-channel events; and *c*, the opening probability histogram, a plot in which entries were made at the time of each opening transition during an interval following a closing to the baseline. Quantitative expressions for the three probabilities that describe these histograms will be presented below; their complete derivations can be found in Dionne and Leibowitz (10).

The open-duration histogram represents the distribution of measured single-channel open lifetimes. In a formal sense this histogram describes the probability $p_1(t)$ of an open channel closing, conditioned upon opening at time zero. With respect to scheme 1 the probability may be written as $p_1(t) = \alpha\,\Delta t\,\exp[-\alpha t]$. The actual expression $P_1(t)$, which we have used to describe our experimental open-duration histograms, incorporated two additional factors: the number of entries in the histogram (N) and the minimum accepted open duration ($2\Delta t$).

$$P_1(t) = N\,\alpha\,\Delta t\,\exp[-\alpha(t - 2\Delta t)]. \qquad (2)$$

In this expression α is the only unconstrained parameter; it has been evaluated by fitting $P_1(t)$ to the open duration histogram using a maximum likelihood method. This method is statistically reliable and fast to compute, although it lacks the robustness of a nonlinear regression (10). Unresolved brief closed intervals, which must certainly have corrupted some of the open durations used in the histogram, were not considered in deriving $P_1(t)$. The corrections to α necessitated by this omission will be discussed later.

The first-latency histogram represents the distribution of closed (baseline) intervals between open channels. Formally it describes the joint conditional probability $P_2(t)$ with which an opening transition occurs at time t conditioned upon both a closing transition at time zero and no opening in the interval $(0,t)$. With respect to scheme 1, this probability may be written explicitly as

$$P_2(t) = \beta\{\bar{n} + \exp[-(\beta + k_{-2})t]\}.$$

$$\exp(-\beta\bar{n}t - \frac{\beta}{\beta + k_2}\{1 - \exp[-(\beta + k_{-2})t]\})\Delta t. \quad (3)$$

The time course of $P_2(t)$ is shown by the theory in Fig. 8. The function is nonlinear and is more complex than the sum of three exponential terms. There are three parameters in this expression, the two rate constants β and k_2 as well as $\bar{n}$, the equilibrium occupancy of the closed state A_2R. Only the rate constants have been estimated by fitting $P_2(t)$ to the first latency histogram. The occupancy of A_2R, $\bar{n}$, was evaluated independent of the transition rate constants using the time-independent portion of $P_3(t)$ as described below.

The opening-probability histogram represents the distribution of channel openings during a time period following a closing transition to the baseline. Formally it describes the conditional probability $P_3(t)$ of opening transitions occurring conditioned upon a closing to the baseline at time zero. With respect to scheme 1, $P_3(t)$ may be written as $P_3(t) = \beta\, n(t)\, \Delta t$ where $n(t)$ is the time-dependent occupancy of the A_2R state. Solving scheme 1 explicitly for $n(t)$ leads to the expression below which we have used to describe the experimental opening probability histograms.

$$P_3(t) = \beta\bar{n}\Delta t + \beta\,[A_1 \exp(-a_1 t) + A_2 \exp(-a_2 t)]\Delta t \quad (4)$$

$$A_1 = \frac{(a_1 - \alpha)(a_1 - \epsilon)}{a_1(a_1 - a_2)}$$

$$A_2 = \frac{(\alpha - a_2)(a_2 - \epsilon)}{a_2(a_1 - a_2)}$$

$$a_{1,2} = \tfrac{1}{2}\,[(\alpha + \beta + k_{-2} + \epsilon) \pm \{(\alpha + \beta + k_{-2} + \epsilon)^2 - 4(\alpha k_{-2} + \alpha\epsilon + \beta\epsilon)\}^{1/2}] \quad (5)$$

$$\bar{n} = Nc^2 k_1 k_2 / k_{-1} k_{-2}$$

$$\epsilon = k_2 c^2 / (c + k_{-1}/k_1)$$

$P_3(t)$ is the sum of two exponential components and a constant. Here A_1 and A_2 are the amplitudes of the exponential terms, a_1 and a_2 are the low-concentration apparent rates for the kinetic scheme, $\bar{n}$ is the equilibrium occupancy of the closed state A_2R, and ϵ is the normalized forward binding rate (units: s^{-1}). The time course of $P_3(t)$

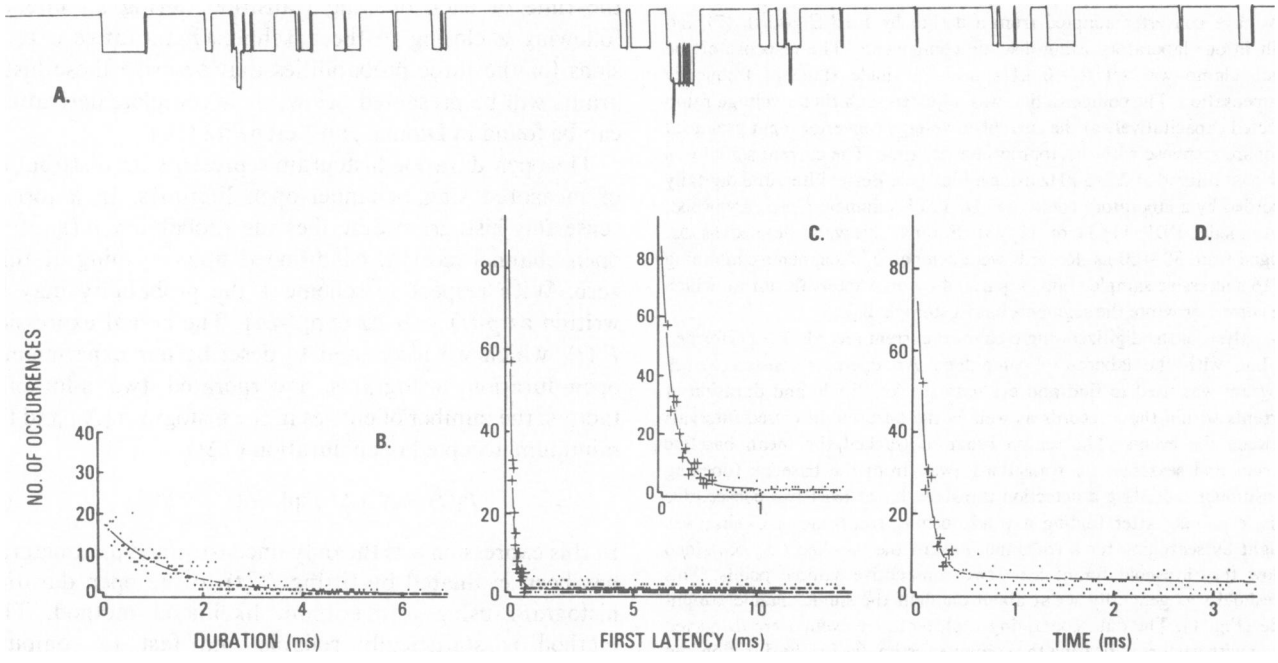

FIGURE 2 Synthesized single-channel data. *A*, ~200 ms of synthesized record from 100 hypothetical channels. *B*, the distribution of measured "open durations" for 727 events resolved using the computer event detection program, fit by maximum likelihood with a single exponential decay rate of 813 s^{-1}. The rate used to generate the data was 800 s^{-1}. *C*, the first latency histogram for the same record, containing 761 entries, fit with Eq. 3 using values of 3,600 and 6,000 s^{-1} for β and k_{-2}. The values used to generate the data were 3,000 and 5,000 s^{-1}. The first 16 data points have been plotted as cursors for clarity. *Inset*, the first 2 ms with an expanded scale. *D*, the opening probability histogram for the same record fit with Eq. 4 using the values for α, β and k_{-2} given above; 743 entries, $\beta\bar{n}$ = 107 s^{-1}. The bin width for all histograms was 30 μs. The first 11 data points have been plotted as cursors for clarity. In all cases the axes have been shifted away from zero so that the data would not be obscured.

is shown by the theory in Fig. 9. This function exhibits a rapid decay, beginning at time zero and ending at an nonzero level which reflects the equilibrium occupancy of A_2R.

In practice, we used the time-independent portion of $P_3(t)$ to evaluate the product $\beta\bar{n}$ and combined this with the expression for the first latency histogram, $P_2(t)$, to estimate β and k_{-2}. The resulting estimates for β and k_{-2} determined in this way were in turn used to predict the time-dependent part of $P_3(t)$, thereby demonstrating the consistency of the fitted transition rates. By reducing the number of free parameters in each fitting procedure, the standard errors of the estimates obtained were reduced. For both $P_2(t)$ and $P_3(t)$ the quality of fit to the data was judged by eye.

The precise expression shown here for $P_3(t)$ is slightly modified from that presented earlier (10). In that earlier expression for $P_3(t)$, we set ϵ equal to zero, while here we use an estimated value for ϵ to produce a more accurate description of the data. This change has resulted in no significant differences in our estimates of β and k_{-2}.

RESULTS

We evaluated the accuracy of transition rate constants estimated by single-channel ensemble analysis using synthetic single-channel records generated according to scheme 1. To produce the synthetic data, values were assigned for each of the six transition rate constants and for the agonist concentration. From these the probability densities of each possible transition within the scheme were calculated. A computer program synthesized the data by monitoring the state in which each hypothetical AChR resided. At 5 μs-increments the computer selected random numbers to determine, for each channel, whether a transition to a new state had occurred based upon the probability for that transition. Every 30 or 100 μs a "sample" was taken in which the number of "open" AChR was recorded. These synthetic raw data records were analysed in a manner identical to that described earlier for experimental data. The analysis of a simulation using 100 hypothetical channels is shown in Fig. 2. In this example the estimates of the three rate constants were: α, 813; β, 3,600; and k_{-2}, 6,000 s^{-1}, compared with their respective assigned values of 800, 3,000, and 5,000 s^{-1}. These estimates are uncorrected in the sense that all brief open and closed intervals of less than two sample intervals were ignored. The systematic bias that this introduces will be addressed in the discussion section below.

TABLE I
ANALYSIS OF SYNTHESIZED DATA

	1 Channel		100 Channels	
	30μs	100μs	30μs	100μs
α	726	588	810	637
β	3,800	3,000	3,600	2,400
k_{-2}	5,800	5,000	6,000	6,500

The single-channel ensemble method was used to analyse computer generated single-channel data as described in the text. The tabulated values are the estimates obtained when the sample interval was 30 or 100 μs, and there were either 1 or 100 hypothetical channels in the 'patch'. The expected values for α, β, and k_{-2} were 800, 3,000, and 5,000 reciprocal seconds.

The results from this and three other simulations are presented in Table I. These simulations represent a range of synthetic conditions, starting with the same input transition rate constants. Simulations were produced for "patches" containing either one or 100 hypothetical channels with samples taken at either 30 or 100 μs intervals. The quality of these uncorrected estimates supports the

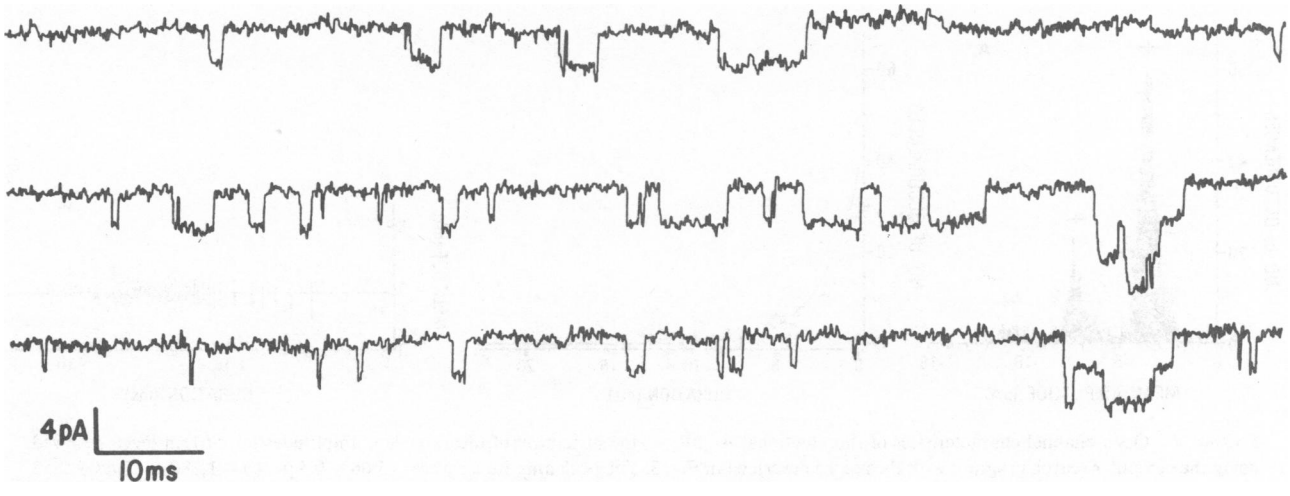

FIGURE 3 Junctional acetylcholine receptor single-channel currents. Three contiguous segments of single-channel data selected to show both single and multiple events. This 0.4 s section was selected from a 14.75 s record sampled at 100 μs intervals in the presence of 500 nM acetylcholine at room temperature. The pipette potential was 47 mV and the membrane potential was −92 mV. Low-pass filtered at 4 kHz.

accuracy of the transition rate constants obtained using single-channel ensemble analysis.

Junctional AChR Records

In the presence of low concentrations of ACh or carbamylcholine (CCh), digital records of junctional transmembrane current contained numerous events identified as single-AChR–channel currents as well as less-frequent instances during which more than one AChR channel was open. An example of such a record elicited with 500 nM ACh is shown in Fig. 3. The amplitude histogram for this record (Fig. 4 *A*) was characterized by open-channel amplitudes that were multiples of a unitary amplitude (here, −3.7 pA). The peaks appear to be Gaussian and the number of observations at each level decreased approximately exponentially as the current levels increased. These observations are consistent with the assumption that the patch contained a large homogenous population of independent AChR channels. This contention is further supported by the distribution of open-channel lifetimes (Fig. 4 *B*) that fitted a single exponential with a decay rate of 455 s^{-1}. Plotting single-channel open duration vs. amplitude for each unitary event (Fig. 4 *C*) indicated that the amplitudes of the briefer events accepted during analysis were not systematically attenuated, although the variance around the mean current increased as event duration decreased.

For cell-attached patches the resting membrane potential was estimated using single-channel current voltage (*I-V*) relationships (Fig. 5). The single-channel *I-V* relation was linear, allowing the conductance to be estimated as the slope of the regression line. Because the reversal potential for the AChR has been shown to be unaffected by temperature (14) or enzyme treatment, the resting potential was estimated from the zero current intercept. In this example the single-channel conductance was 43 pS and the resting potential was −45 mV. A cumulative *I-V* plot using

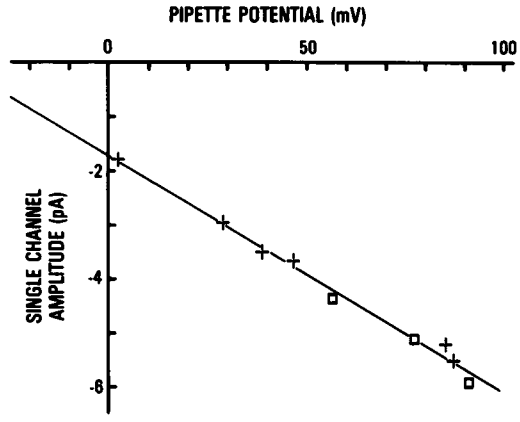

FIGURE 5 Single-channel current as a function of pipette potential. The mean single-channel current was plotted as a function of pipette potential for channels activated with 500 nM ACh (+) or 10 μM CCh (□) on one cell. Positive pipette potentials hyperpolarize the membrane patch. The line has been fit by a linear least-squares regression which gave a slope conductance of 43 pS, a zero current intercept of −40 mV and a correlation coefficient of −0.995, at room temperature. Using −5 mV as the reversal potential for the junctional AChR (13), the resting potential of this cell was −45 mV.

data from 16 patches from four cells, at room temperature, is shown in Fig. 6. The single-channel conductance of 42 pS was constant for channels activated with either ACh or CCh. In a few instances, for other cells, single channels were recorded at only one potential. In these cases this conductance (42 pS) was used to estimate the resting potential.

The open-duration histograms provided a direct estimate of the channel-closing rate constant, α. For channels activated with 500 nM ACh or 10 μM CCh at room temperature, α varied as a function of voltage (Fig. 7). The magnitude of this voltage dependence (173 mV for an *e*-fold change with ACh and 181 mV with CCh) was not significantly different for either agonist, although the

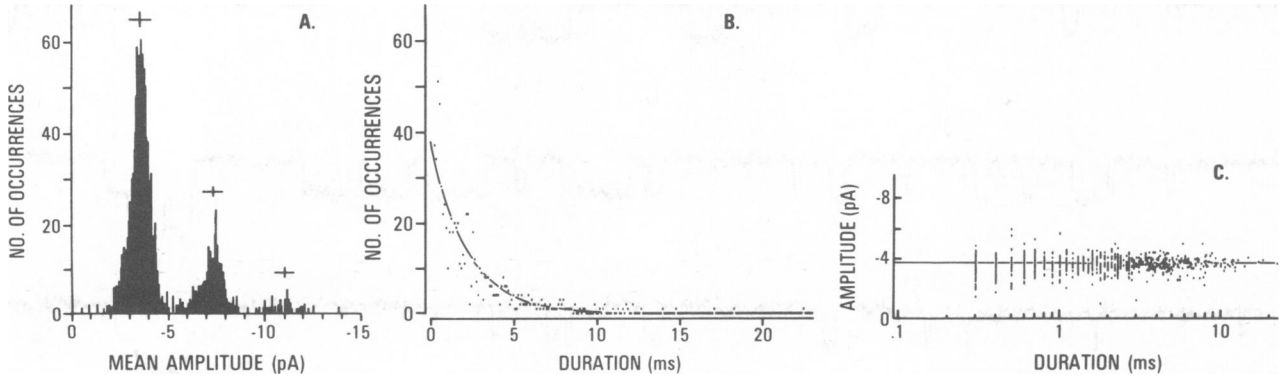

FIGURE 4 Open-channel characteristics of the junctional AChR. *A*, the histogram of mean current amplitudes for current levels resolved using the computer search program with the record described in Fig. 3. The peak amplitudes were −3.66 ± 0.5 pA (n = 1,280); −7.48 ± 0.53 pA (n = 336); and −11.16 ± 0.59 pA (n = 54). The vertical line above each peak indicates the mean current; the horizontal cross bar indicates the standard deviation. *B*, the single-channel open-duration histogram for the record fit with a single exponential function with a time constant of 455 s^{-1}. The minimum event duration accepted was 300 μs. *C*, a plot of single-channel current amplitude vs. duration for each of the 788 single events. The mean current (3.7 pA) is shown by a horizontal line.

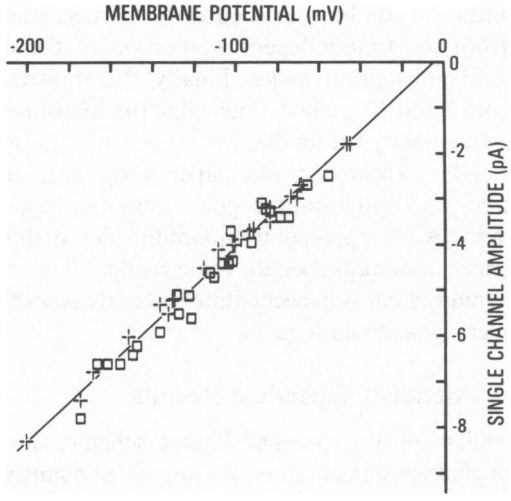

FIGURE 6 Single-channel current as a function of membrane potential. The mean single-channel current from 16 patches derived from four cells recorded at 49 potentials were plotted as a function of transmembrane potential. Channels activated with 500 nM ACh (+, $n = 23$) or 10 μM CCh (□, $n = 26$) have the same single-channel slope conductance, 42 pS and reversal potential. The line was fit using a linear least-squares regression with a correlation coefficient of 0.988.

closing rate for ACh at any voltage was smaller than that for CCh.

Estimates of the rate constants β and k_{-2} were obtained by fitting both conditional probability functions described earlier, $P_2(t)$ and $P_3(t)$, to the appropriate histograms. The first latency histogram (Fig. 8) displayed a complicated time course which was accurately described by the probability function $P_2(t)$. In the example in Fig. 8, for channels activated by 500 nM ACh at a membrane potential of -92 mV, estimates for β and k_{-2} were 1,200 and 3,200 s^{-1}. For the opening-probability histogram (Fig. 9) the probability

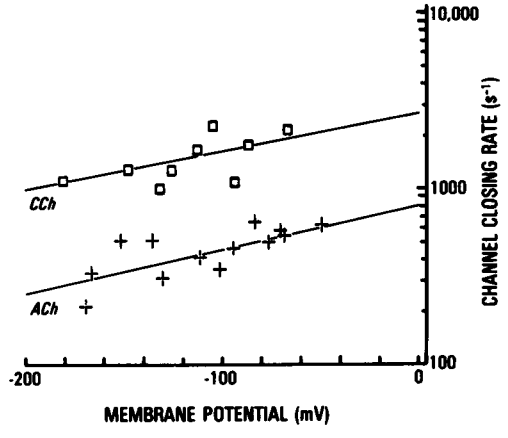

FIGURE 7 Channel-closing rate as a function of membrane potential. The channel closing rate (α), determined using open-duration histograms, was plotted as a function of membrane potential for channels activated with 500 nM ACh (+) or 10 μM CCh (□). The lines have been fit using a linear least-squares regression. For ACh the voltage dependence was equivalent to an e-fold change in 173 mV, while for CCh 181 mV were required; the correlation coefficients were 0.719 and 0.621.

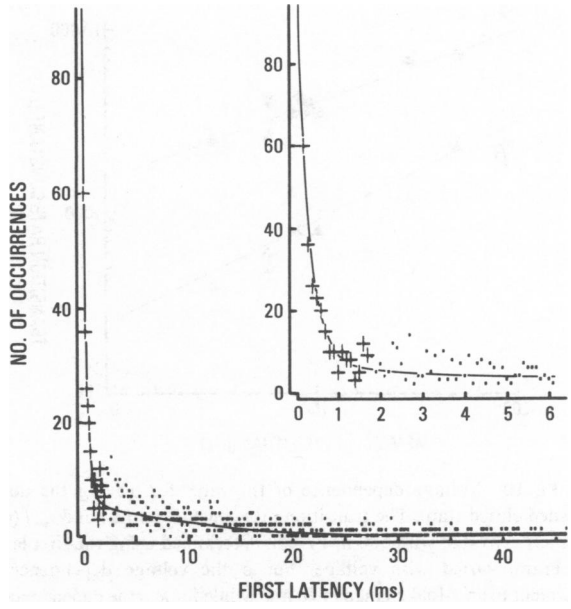

FIGURE 8 The first-latency histogram. The first-latency histogram for the record described in Fig. 3 was fit with Eq. 3. $\beta = 1{,}200\ s^{-1}$, $k_{-2} = 3{,}200\ s^{-1}$, $\alpha = 455\ s^{-1}$, and $\beta\bar{n} = 92\ s^{-1}$, 972 entries and 100 μs bins. Note that the axes have been shifted away from zero so that they do not obscure the data. The first 16 points have been plotted as cursors for clarity and the *inset* shows the first 6 ms with an expanded time scale.

$P_3(t)$, shown as a solid line, described the data well, using the values for β and k_{-2} evaluated from $P_2(t)$. Values for β and k_{-2} obtained in the presence of 500 nM ACh were potential dependent (Fig. 10). These dependencies, 78 mV for an e-fold change in β and 105 mV for an e-fold change

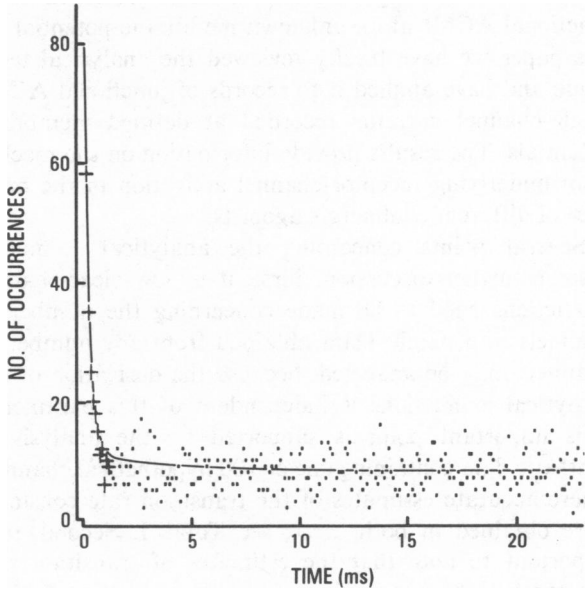

FIGURE 9 The opening-probability histogram. The 25 ms opening-probability histogram for the record described in Fig. 3 was fit with Eq. 4. For values of the transition rate constants see Fig. 8. The axes have been shifted away from zero so that they do not obscure the data. The first 11 points have been plotted as cursors for clarity.

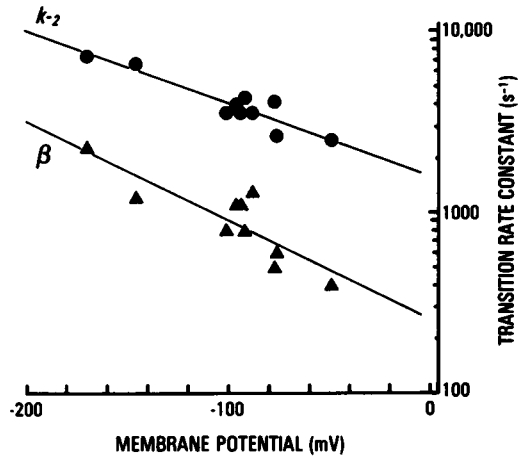

FIGURE 10 Voltage dependence of the rates for leaving the doubly-liganded closed state. The transition rate constants β (▲) and k_{-2} (●) for channels activated with 500 nM ACh, determined using the first latency histogram, varied with voltage. For β the voltage dependence was equivalent to an e-fold change in 78 mV, while for k_{-2} the dependence was 105 mV. The lines were fit using a linear least-squares regression; the correlation coefficients were −0.856 for β and −0.933 for k_{-2}.

in k_{-2}, were not statistically different in magnitude and caused the rates to increase with hyperpolarization. When CCh was used to activate junctional AChR at room temperature, the fast components of the first latency and opening probability histograms were not resolved.

DISCUSSION

Single-channel ensemble analysis was described in detail by Dionne and Leibowitz in 1982 (10). That report presented the mathematical basis of the method and was illustrated with single-channel currents obtained from junctional AChR at an unknown membrane potential. In this paper we have briefly reviewed the analytical technique and have applied it to records of junctional AChR single-channel currents recorded at defined membrane potentials. The results provide information on the mechanism underlying receptor-channel activation in the presence of different cholinergic agonists.

Several points concerning the analytical technique deserve further discussion. First, it is now clear that no restrictions need to be made concerning the number of channels in a patch. Data obtained from any number of channels may be analyzed, because the derivation of the analytical expressions is independent of this parameter. This important point is supported by the analysis of synthetic data containing one or 100 hypothetical channels where accurate estimates of the transition rate constants were obtained in both cases; see Table I. Second, it is important to note that the estimates of transition rate constants were obtained in a manner that minimized propagation errors. Specifically, the evaluation of α, β, k_{-2} and $\bar{n}$ were, to some degree, independent of each other. The channel-closing rate constant, α, was obtained from the open-duration histogram directly, while $\beta\bar{n}$, the opening rate times the equilibrium occupancy of A_2R, was evaluated from the time-independent portion of the opening probability histogram alone. Finally the transition rate constants β and k_{-2}, which determine the lifetime of A_2R, were evaluated by fitting the first latency histogram.

The data presented in this paper were analyzed using both two- and three-sample–point minimum open durations and two-sample–point minimum closed durations. The longer minimum open duration reduces the resolution of the analysis but was necessitated in early recordings by the lower signal-to-noise ratio.

Model-Independent Results

Independent of any assumed kinetic scheme, the results presented above demonstrate two important points relating to ion permeation through the junctional AChR channel. First, the single-channel conductance, γ, is the same for channels activated with either ACh or CCh for the membrane potential range of −40 to −200 mV. Earlier estimates of endplate single-channel conductance made using noise analysis (15) produced different values of γ for different agonists. This may have been caused by an inappropriate evaluation of the spectral density, which was markedly non-Lorentzian for two of the synthetic agonists used. Indeed, as we have discussed before (10, 12), the expected power spectrum produced using scheme 1 would contain at least two Lorentzian components, although the faster, smaller component might not have been well resolved in most early noise studies. Second, the reversal potentials for channels activated with either of the two agonists used were identical (Figs. 5, 6). This indicates that the properties of the channel that determine ion permeation are the same for these two agonists and may be so in general. Indeed, similar findings have been reported for glutamate-activated channels in locust muscle (16).

Model-Dependent (Kinetic) Results

We have applied single-channel ensemble analysis to recordings of endplate AChR single-channel currents to evaluate the kinetic transition rate constants α, β, and k_{-2} using scheme 1. For channels activated with ACh, the voltage dependence of all three rates has been investigated. In addition, for channels activated with CCh, the channel-closing rate, α has been directly estimated and an indirect estimate has been made for the channel-opening rate constant β. The closing rate constants for channels activated with these two agonists were different at all potentials examined, although the voltage dependencies of the rates were agonist independent. Earlier we reported similar values for the closing rate constant α with the two agonists ACh and CCh (10); those values, however, were obtained on different cells at unknown membrane potentials. For junctional channels activated with 500 nM ACh, both β and k_{-2} exhibited voltage dependencies of the same sign and similar magnitude, causing the rates to increase e-fold

for ~92 mV of hyperpolarization. The voltage dependencies of β and k_{-2} result in a voltage-dependent lifetime for the closed, doubly-liganded state, A_2R, which decreases with hyperpolarization.

All of the analysis discussed has assumed that the resolved data represented a complete and accurate record of all opening and closing transitions. Because this assumption is formally invalid, it was important to estimate the degree of contamination by missed transitions as well as the effect of such omissions on the estimates of transition rate constants. In an earlier report (10) we presented a quantitative discussion of this problem. There we calculated the expected number of brief openings and closings that might be missed and could distort the estimates of the rate constants. It was concluded that the projected errors in the estimates for α, β, and k_{-2} were <25%. Here we have approached the issue by generating synthetic data using known transition rate constants to test the analytical method. This test produced good estimates of the rate constants with a similar margin of error, and showed that the analysis is insensitive to the number of channels generating the data. Two factors dominated the error in these estimates. First, unresolved transitions bias the histograms by distorting the distributions: some time segments that appeared to be single openings and closings were in reality several shorter openings or closings. Second, resolved multiple events were not included in the open-duration histogram and therefore bias the estimate of α to shorter values because longer events were more likely to be included in multiple events than shorter ones. (This factor was of little significance because the proportion of multiple events in any data set was small.)

An indirect estimate of the channel-opening rate constant β for CCh-activated channels has been obtained from the equilibrium frequency of channel opening, although neither the time-dependent portion of the opening probability histogram nor the fast component of the first latency histogram could be resolved using this agonist. The equilibrium frequency is just the time-independent portion of the opening probability histogram, $\beta\bar{n}$. We have used β and $\beta\bar{n}$ from data recorded with ACh to estimate an average value for N, the number of receptors in a patch. Together with an estimate of the CCh equilibrium dissociation constant (300 μM), we have calculated $\bar{n}$ for the CCh-activated channels. Using this and the experimentally determined value for $\beta\bar{n}$ with CCh, we have estimated β for CCh-activated channels. This procedure produced an average opening rate constant of ~250 s^{-1} for channels activated with CCh. We believe that the standard deviation associated with this estimate is at least 100%. Nevertheless, this approximation for β is of the same magnitude as the value experimentally determined for channels activated with ACh at a transmembrane potential of -100 mV (~900 s^{-1}) and not an order of magnitude larger.

Qualitatively, the probability of channel opening must be lower for channels activated with CCh than with ACh, because a higher concentration of agonist, relative to its equilibrium dissociation constant, was needed to produce a similar rate of openings. Because frequent channel openings were not observed shortly after closings, it appears that channels were less likely to open even when doubly-bound with CCh. Quantitatively, the probability that a transition out of the A_2R state will be an opening transition, $\beta/(\beta + k_{-2})$, may be smaller for CCh than for ACh. Because β seems to be roughly equal for the two agonists, the difference must result from a change in k_{-2}.

Although the above approximations for β with CCh indicate that the kinetic differences between CCh- and ACh-activated channels are determined for the most part by changes in the unbinding rate constant, k_{-2}, it is important to measure the transition rate constants for CCh directly. The most productive approach to resolving the fast kinetics of CCh-activated channels will probably be to study them at low temperature. To understand the activation kinetics of the AChR it will be necessary to examine a complete range of temperatures using a series of agonists.

We have estimated three of the transition rate constants for AChR channel activation at a vertebrate neuromuscular junction. Several other reports have described single-channel studies of AChR kinetics on extrajunctional membrane (9) and on cultured cells (17–19) where receptor density is comparatively low, but have not reported examination of junctional receptors. Nonjunctional receptors have been reported to show two component distributions of open-channel lifetime (9, 19) and to exhibit several conductance states (17, 18). These properties, which were not apparent in our records, indicate that the activation kinetics of nonjunctional receptors may be more complicated than scheme 1; however, the precise nature and source of this complexity is unclear. It is possible that each nonjunctional receptor displays a different, more complicated behavior than that shown by junctional receptors or that extrajunctional receptors are of two or more kinds, each with a different kinetic behavior.

We would like to thank Scott Thomson, Dick Horn, and Joe Henry Steinbach for helpful discussion.

This work was supported by National Institutes of Health grant NS 15344, and Office of Naval Research contract N00014-79-L-079.

Received for publication 2 May 1983 and in final form 13 June 1983.

REFERENCES

1. Fatt, P., and B. Katz. 1951. An analysis of the end-plate potential recorded with an intra-cellular electrode. *J. Physiol.* (*Lond.*). 115:320–370.
2. Adams, P. R. 1981. Acetylcholine receptor kinetics. *J. Membr. Biol.* 58:161–174.
3. Steinbach, J. H. 1980. Activation of nicotinic acetylcholine receptors. *In* The Cell Surface and Neuronal Function. C. W. Cotman, G. Poste, and G. L. Nicolson, editors. Elsevier/North-Holland Biomedical Press, Amsterdam. 119–156.
4. Magleby, K. L., and C. F. Stevens. 1972. A quantitative description of end-plate currents. *J. Physiol.* (*Lond.*). 223:173–197.

5. Anderson, C. R., and C. F. Stevens. 1973. Voltage clamp analysis of acetylcholine produced end-plate current fluctuations at frog neuromuscular junctions. *J. Physiol.* (*Lond.*). 235:655–691.
6. Neher, E., and B. Sakmann. 1976. Single channel currents recorded from membrane of denervated frog muscle fibres. *Nature* (*Lond.*). 260:799–802.
7. Hamill, O. P., A. Marty, E. Neher, B. Sakmann, and F. J. Sigworth. 1981. Improved patch-clamp techniques for high-resolution current recording from cells and cell-free membrane patches. *Pflügers Arch. Eur. J. Physiol.* 391:85–100.
8. Colquhoun, D., and A. G. Hawkes. 1981. On the stochastic properties of single ion channels. *Proc. R. Soc. Lond. B. Biol. Sci.* 211:205–235.
9. Colquhoun, D., and B. Sakmann. 1981. Fluctuations in the microsecond time range of the current through single acetylcholine receptor ion channels. *Nature* (*Lond.*). 294:464–466.
10. Dionne, V. E., and M. D. Leibowitz. 1982. Acetylcholine receptor kinetics, a description from single-channel currents at snake neuromuscular junctions. *Biophys. J.* 39:253–261.
11. Del Castillo, J., and B. Katz. 1957. Interaction at end-plate receptors between different choline derivatives. *Proc. R. Soc. Lond. B. Biol. Sci.* 146:369–381.
12. Dionne, V. E. 1981. The kinetics of slow muscle acetylcholine-operated channels in the garter snake. *J. Physiol.* (*Lond.*). 310:159–190.
13. Kuffler, S. W., and D. Yoshikami. 1975. The number of transmitter molecules in a quantum: an estimate from iontophoretic application of acetylcholine at the neuromuscular synapse. *J. Physiol.* (*Lond.*). 251:465–482.
14. Hoffman, H. M., and V. E. Dionne. 1983. Temperature dependence of ion permeation at the endplate channel. *J. Gen. Physiol.* 81:687–703.
15. Colquhoun, D., V. E. Dionne, J. H. Steinbach, and C. F. Stevens. 1975. Conductance of channels opened by acetylcholine-like drugs in muscle end-plate. *Nature* (*Lond.*). 253:204–206.
16. Gration, K. A. F., J. J. Lambert, R. L. Ramsey, R. P. Rand, and P. N. R. Usherwood. 1981. Agonist potency determination by patch clamp analysis of single glutamate receptors. *Brain Res.* 230:400–405.
17. Hamill, O. P., and B. Sakmann. 1981. Multiple conductance states of single acetylcholine receptor channels in embryonic muscle cells. *Nature* (*Lond.*). 294:462–464.
18. Auerbach, A., and F. Sachs. 1983. Flickering of a nicotinic ion channel to a subconductance state. *Biophys. J.* 42:1–10.
19. Jackson, M. B., B. S. Wong, C. E. Morris, H. Lecar, and C. N. Christian. 1983. Successive openings of the same acetylcholine receptor channel are correlated in open time. *Biophys. J.* 42:109–114.

DISCUSSION

Session Chairman: Harold Lecar *Scribes*: James Lechleiter and Robert A. Maue

LECAR: The number of channels in a patch has been a problem. You have produced a method that works with N channels and provides an estimate of the number of channels in the patch. Would you explain further?

DIONNE: Kinetic rates can be derived in a straightforward fashion if one assumes only one channel per patch. Unfortunately that is not always a valid assumption. The trouble is that with more than one channel, you can't make that assumption. We decided to treat the system in a manner similar to perturbation analysis. In any kinetic study you perturb the system, try to populate a specific state and then watch how the system relaxes back to equilibrium.

When a channel closing occurs, the population of the specific doubly-liganded state from which opening occurs is perturbed and incremented by one. As long as that perturbation is large compared with the average occupation of that closed state, one can watch how its population relaxes. At low agonist concentrations, the average occupation of that state ($\bar{n}$), is on the order of 0.01 to 0.1 (i.e., usually there are no channels there). The population of this state decays exponentially as

$$n(t) = \bar{n} + \exp(-\kappa t)$$

where κ is the lifetime. The constant $\bar{n}$ is proportional to the total number of channels in the patch, but it is small because of the low agonist concentration.

AUERBACH: Because you work on a synaptic preparation, you have the opportunity to test the model you use by checking whether the rate constants you get from the single channel data agree with the macroscopic results. With regard to this, I wonder about two apparant discrepancies. First, the amplitude and rise time of miniature end plate currents (mepc) require that ~1,500 channels open in ~200 μs. I estimate that this requires that ~40,000 molecules of acetylcholine are in a quantum, assuming that the entire rise time is due to the opening process and there are no binding or diffusional delays . Using the results of Land, Salpeter, and Salpeter (1981. *Proc. Natl. Acad. Sci. USA.*), I estimate that 60,000–80,000 molecules of ACh would be required. That seems to be high. Second, the mean lifetime of your bursts of current seem to be only mildly voltage dependent, whereas your results on the macroscopic currents in the same preparation show a much greater voltage dependence. Is it possible that your enzyme treatment is responsible for this difference?

DIONNE: If you take the rates that we have given and assume the low concentration limit, the predicted time course of the mepc rise time is too slow, being delayed by as much as 2 ms. However, the mepc is produced by a brief but high agonist concentration. This would tend to shorten the rise time. Because I can't measure the time course of the concentration change, I don't know whether one can account for the entire discrepancy between the predicted and the observed time courses on this basis.

The enzymatic treatment that we use for our preparation may damage or alter the kinetics of the system. We must treat the muscle with a combination of protease and collagenase to remove the nerve terminal and enough of the basement membrane to allow seal formation to the patch electrode. Although the proteases may nick the AChR protein, biochemical flux studies done in Lindstrom's lab do suggest that the protease-treated AChR protein remains functional. We don't know whether the protein continues to work in precisely the same fashion or with the same kinetic rates. One indication that it may not is the different voltage dependencies of the kinetic rates estimated using macroscopic measurements (e.g., noise analysis) in this system compared to estimates derived from the microscopic measurements (single channel analysis.) Part of this discrepancy may be due to the fact that the macroscopic time course and spectral corner frequency reflect more than just α. We have not done noise analysis and patch recordings on the same end plate after it has been enzymatically denervated, although that would be an interesting experiment. Unfortunately, after these cells are treated enzymatically to remove the nerve terminals, microelectrode impalement tends to cause very rapid cell death, making macroscopic measurements difficult to obtain. On the other hand, patch recording is tolerated well.

SACHS: In the paper you discussed the number of channels in the patch, but didn't state how you got that number. Is that the number in the

absence or presence of desensitization and are those numbers in agreement with toxin binding at the same end plate?

DIONNE: α-bungarotoxin does not bind to these receptors. The numbers come from the opening probability, $P_3(t)$ (Fig. 9), which decays rapidly until it reaches an equilibrium value. $\beta \times \bar{n}$ is evaluated by fitting the time-independent component of the curve. This gives on the order of 100–1,000 channels in these patches, which does not seem excessive considering the densities that have been estimated in other preparations using radioactive toxins.

SACHS: Using numbers often given for the channel densities, such as $10{,}000/\mu m^2$, and the estimates we and the Göttingen group have made for patch area (2–10 μm^2), there should be a zillion channels.

DIONNE: I don't know if we have 10-μm^2 patches; I would doubt it.

SACHS: So is that estimate of N only that fraction that has not desensitized?

DIONNE: That could be a desensitized level. However, in most cases, we don't see major changes in the rate of channel activity that would indicate the onset of desensitization. Although 0.5 μM ACh can cause desensitization in some culture systems, here, at the end plate, it doesn't appear to do so.

SACHS: In principle, your analysis allows for an arbitrarily large number of channels as long as the time constants for the repeated openings are separate from the times between presumably independent openings. Although this is a slightly different formulation from the one Colquhoun and Hawkes developed, you both measure the same properties and both depend on having the same separation of the time-dependent part from the time-independent part. Therefore, if you took your data and treated it with their analysis you would have to get the same answers.

DIONNE: We have not applied Colquhoun and Hawkes' method of analysis to our data. Their analysis is based upon the very strong assumption that two successive openings can be attributed to the same or different channels with a fair reliability. If there is a long quiet period between the openings, then they attribute the openings to different channels, while bursts of openings are attributed to the same channel. The records that we obtain at the snake end plate do not show isolated bursts of activity.

SACHS: But you have that time-dependent component of the opening probability within the first few 100 μs. Apparently, your dissociation rate is fast enough that you don't see much repeated activity and there may be only 1.1 events per burst in the data.

DIONNE: As I mentioned, we have not applied their method of analysis to our data because of the large numbers of channels, and therefore I can't say whether we would get the same numbers using Colquhoun and Hawkes' analysis. What we have done is test our analytic approach using synthetic computer-generated data. We find good agreement between the estimates obtained from single channel ensemble analysis and the numbers used to produce the synthetic data.

PATLAK: I have data from both frog and snake end plates that address an earlier question of Fred Sachs' regarding channel density. With 0.5 μM ACh, when the patch electrode first touches a frog synapse, you see a tremendous noise response with no discernible single channel currents. In contrast, during the first touch to snake synapses, individual channel currents are observed. Since K_d for these two preparations are not orders of magnitude different, I think your estimate of 100–1,000 channels per patch is comforting.

In your manuscript, the voltage dependence of β and of k_{-2} is approximately parallel. Am I correct in interpreting these data to mean that the average length of the burst would not be changing because of the voltage dependence of β and k_{-2}, but rather because of the voltage dependence of α?

DIONNE: Yes. The voltage dependencies of those rate constants are similar. Thus the lifetime of the doubly liganded closed state will decrease with hyperpolarization while β increases. This leaves the burst length largely insensitive to voltage.

PATLAK: Does that turn out to be in the direction that explains the discrepancy between your microscopic α and the voltage dependence that you would measure in a macroscopic sense?

DIONNE: Yes, but it is not enough to explain the differences.

MISLER: Concerning the intactness of the receptor channel, have you tried to examine mepc before and after denervation using a method iontophoresis similar to that of Kuffler and Yoshikami (Kuffler, S. W., and D. Yoshikami. 1975. The number of transmitter molecules in a quantum: an estimate from iontophoretic application of ACh at the neuromuscular junction. *J. Physiol. (Lond.)*. 251:465–482)? Reproducibility would at least eliminate the possibility that the enzymatic treatment is causing damage.

DIONNE: No, we haven't done that. What I've done is treat the preparation with both proteases and collagenases so that it is half torn apart (most of the synaptic boutons have come off but not all of them). Under those conditions, noise and mepc recorded from the boutons that remain in place show little difference from untreated preparations.

MISLER: But in that preparation, the mean frequency of mepc would presumably be significantly reduced.

DIONNE: Yes.

MISLER: You might be recording mepc from areas where there are intact boutons.

DIONNE: Yes, under those conditions you can record mepc which are similar to untreated mepc. Thus there seems to be no big change in the macroscopic rates induced by enzymatic treatment.

FINKELSTEIN: My question has to do with the determination of the total number of channels. Why can't you directly determine N at the end of your experiment by giving a large dose of ACh, measuring the macroscopic current that you get, and then dividing the current amplitude by the single channel conductance?

DIONNE: I can only guess what would happen under those conditions. Applying high agonist concentrations would probably cause a rapid onset of desensitization which would reduce the maximum possible current.

FINKELSTEIN: Would it give you a lower limit?

DIONNE: Yes.

LEIBOWITZ: That would be a difficult experiment. It is hard to raise the concentration at tip of the patch pipette rapidly.